IECAG 2021

Proceedings

Diachronic mapping of invasive plants using airborne RGB imagery in a Central Pyrenees landscape (South-West France) †

Hugo Jantzi [1,*], Claire Marais-Sicre [2], Eric Maire [3], Hugues Barcet [1] and Sylvie Guillerme [1]

[1] GEODE UMR 5602, University of Jean Jaurès, CNRS, 31058 Toulouse, France; hugo.jantzi@univ-tlse2.fr (H.J.); sylvie.guillerme@univ-tlse2.fr (S.G.); hugues.barcet@univ-tlse2.fr (H.B.)
[2] CESBIO UMR 5126, CNRS, CNES, University of Paul Sabatier, INRAE, IRD, 31400 Toulouse; claire.marais-sicre@cesbio.cnes.fr (C.M-S.)
[3] LIVE UMR 7362, University of Strasbourg, CNRS, 67000 Strasbourg, France; eric.maire@live-cnrs.unistra.fr (E.M.)
* Correspondence: hugo.jantzi@univ-tlse2.fr
† Presented at the 1st International Electronic Conference on Agronomy, 3–17 May 2021; Available online: https://sciforum.net/conference/IECAG2021

Abstract: The rapid spread of invasive plant species (IPS) over several decades has led to numerous impacts on biodiversity, landscape and human activities. Early detection and knowledge on their spatiotemporal distribution is crucial to better understand invasion patterns and conduct appropriate activities for landscape management. Therefore, remote sensing provides great potential for detecting and mapping the spatial spread of IPS. The study presents a mapping of IPS (*Reynoutria japonica* and *Impatiens glandulifera*) over the last decade, on two sites located in the central Pyrenees in the southwest of France, from very high resolution RGB aerial photographs. A supervised classification based on the random forest algorithm was performed using pixel attributes. The original spectral bands (RGB) were used, to which vegetation indices and textures were added to improve the detection. The classification models yielded a mean prediction accuracy (F-score) of 0.90 (0.87 to 0.92) at the site 1 and 0.87 (0.81 to 0.91) at the site 2. Results show that the expansion of IPS is closely related to the presence of corridors (e.g., roads, power lines) and to environments disturbed by human activity such as land clearing.

Keywords: invasive plant species; land use change detection; very high resolution RGB imagery; machine learning; pixel-based analysis; random forest classifier

Citation: Lastname, F.; Lastname, F.; Lastname, F. Title. *Proceedings* **2021**, *68*, x. https://doi.org/10.3390/xxxxx

Published: date

Publisher's Note: MDPI stays neutral with regard to jurisdictional claims in published maps and institutional affiliations.

1. Introduction

Over several decades, biological invasions by plants have increased considerably leading to numerous impacts on biodiversity, landscapes and human activities as well as significant economic and ecological costs [1]. Often, long-term invasions lead to a drastic change in ecosystem with the structure and functioning alteration due to a significant competition with native species [2]. Thus, invasive plant species (IPS) have become an issue all over the world, to the point that they are considered as one of the major causes of the decline of biodiversity [3].

Early detection and knowledge of their spatio-temporal distribution are crucial to better understand invasion patterns and conduct appropriate activities for landscape management [4]. Therefore, remote sensing (RS) provides great potential for detecting and mapping the spread of IPS [5]. RS high resolution aerial photographs have been widely used since the last decade. However, the detection of IPS can be tricky as it generally requires high spectral and/or spatial submetric resolution images and that plants differ from surrounding species and constitute aggregated and dense populations [6]. In recent years, several studies have provided that RS using hyperspectral sensors and/or very high resolution (VHR) imagery, is an effective tool to detect IPS [5,6].

This study presents a mapping of IPS (i.e., *Reynoutria. Japonica* and *Impatiens glandulifera*), using VHR ortho-rectified RGB aerial photographs, over the last decade in the central Pyrenean foothills. The aims are to: (i) produce an approach for detecting IPS; (ii) characterize their spatio-temporal dynamics; (iii) highlight the environmental and human factors that influence their spread.

2. Materials and Methods

2.1. *Study areas*

The study was carried out on two sites, Salles-et-Pratviel (42°55′29″N – 00°38′58″E) and Cierp-Gaud (42°50′06″N – 00°36′13″E), located along the Pique valley in the central Pyrenees in the southwest of France (Figure 1). The sites, which cover an area ranging from 20 to 44 ha, are entrenched in the Pyrenean foothills. The landscape is composed of meadows and stream banks in the valley bottom while deciduous and coniferous forests as well as some shrubs dominate the hillsides. Agricultural activity is mainly composed of permanent meadows for grazing and forage harvesting.

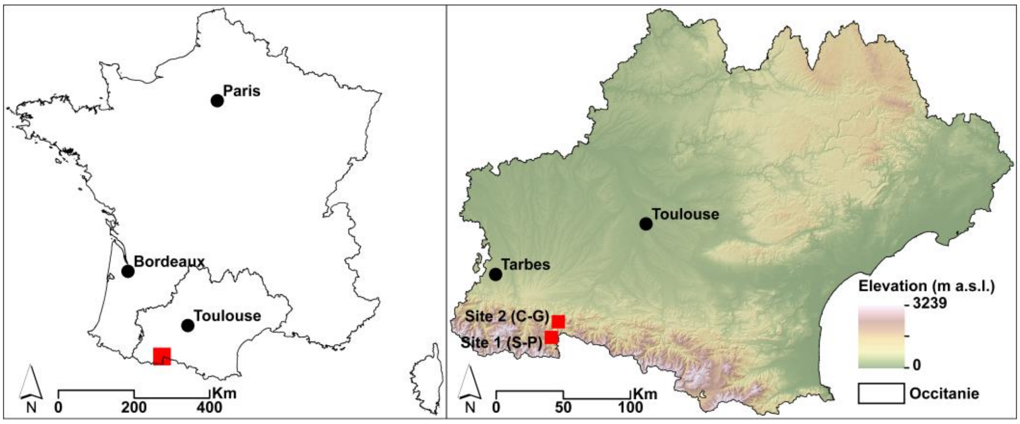

Figure 1. Location map of the study sites. 'S-P', Salles-et-Pratviel; 'C-G', Cierp-Gaud.

2.1. *Target species*

Reynoutria. Japonica Houtt. (Figure 1a) has a highly developed root system composed of rhizomes that produce annual aerial stems up to 3 m in height. Its stems are hollow, reddish and semi-ligneous with marked knots while the leaves are large, oval-triangular and truncated at the base with a sharp point at the apex and creamy-white flowers [7]. *Impatiens glandulifera* Royle (Figure 1b) is a highly annual herb that can reach up to 2.5 m in height with pink flowers and roots reaching a depth of 10-15 cm. Its stems are reddish, multi-branched and hollow with knots. Its leaves are glabrous, oblong, ovate to elliptical and whorled with margins sharply serrated [8]. The two species are preferentially associated with banks and alluvium of streams, as well as on the edge of ditches or areas frequently disturbed.

Figure 2. *Reynoutria japonica* (a) and *Impatiens grandulifera* (b) during the flowering stage.

2.3. *Data collection*

A set of four VHR ortho-rectified RGB aerial photographs were acquired from the National Institute of Geographic and Forest Information (IGN) for each site. Images were taken between July and August and cover the last decade at an interval of 3 years. Their spatial resolution is 20 cm (i.e., 2019, 2016) and 50 cm (i.e., 2013, 2010). Additionally, ground truth data was collected in September 2020 at each site, in order to locate IPS, using a Trimble GEO7X dGPS (Acc.1 cm XY). The data was used for sampling IPS on the images and for field validation of the classification maps. Before 2019, ground truth data was impossible to obtain, therefore Google Street View was used to assess the presence of IPS according to expert opinions in addition to the field data collected.

2.4. *Image data analysis*

The data processing was carried out from Orfeo ToolBox (OTB) which is an open-source project for remote sensing and developed in France by the National Centre for Space Studies (CNES). For this study, OTB was applied through the QGIS software with versions 7.2.0 and 3.14.1, respectively. The workflow of image processing and classification is summarized in Figure 3.

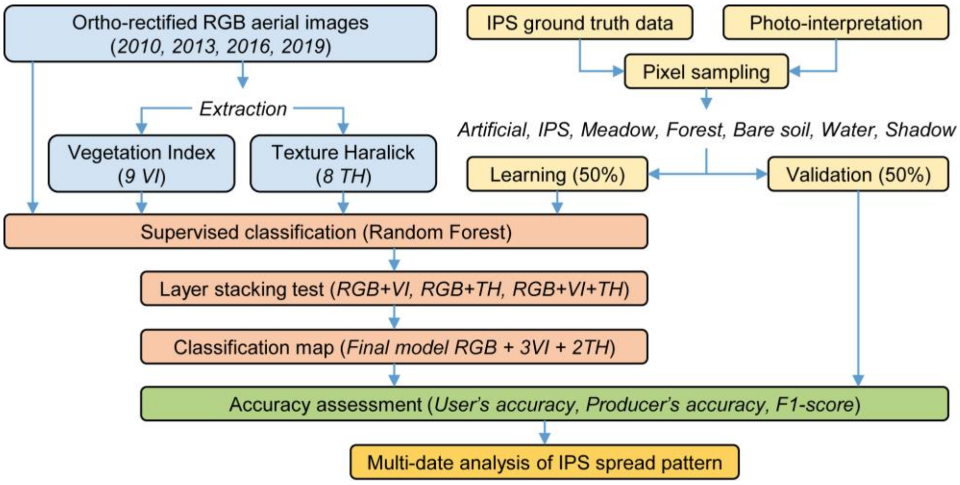

Figure 3. Workflow for RGB imagery processing and analysis of the IPS spatio-temporal dynamics over the last decade**.**

2.4.1. Derived RGB variables

For detecting and mapping IPS, several vegetation indices and texture images were derived from the original spectral bands (RGB). Nine vegetation indices (CIVE, TGI, VDVI, NGRDI, MGRDI, RGBVI, ExG, RGRI) were selected among the most commonly used as well as height textures (Energy, Entropy, Correlation, Inverse Difference Moment, Contrast, Cluster Shade, Cluster Prominence and Haralick Correlation) for each band of the original images [9].

2.4.2. Sample design

To calibrate and validate the classification, seven classes were established (Figure 3). Each class was randomly sampled with ~110 polygons (3 m x 3 m) by photo-interpretation and field survey. In each polygon, a set of points was randomly generated, one point corresponding to one pixel. The total pixel sampling is 20,000 for images at 20 cm resolution and 8,000 for those at 50 cm. If possible, sampling is similar between years. Then, the sampled points were randomly separated into two independent groups to calibrate (50%) and validate (50%) the classifiers.

2.4.3. Image classification

To map IPS, the machine learning algorithm Random Forest (RF) was used in a pixel-based approach [10]. This algorithm is a non-parametric classifier, which combines an ensemble of decision trees in a bagging approach. To assess the benefits of each variable, several classifications were tested according to three levels: (i) the three original bands (RGB); (ii) the benefit analysis where one variable at a time was added to the three original bands; (iii) the combination of variables with the best performance added to the three original bands.

2.4.4. Classification accuracy assessment

Classification accuracy was evaluated from a confusion matrix calculated from the class assignments. The performance criteria selected to assess the classification accuracy are the User's Accuracy (UA), Producer's Accuracy (PA) and F1-score (F1) [11]. PA corresponds to the frequency at which the real features on the field are correctly represented on the classified map while UA corresponds to the frequency at which the class on the map is actually present in the field. F1 combines UA and PA and corresponds to their harmonic mean.

3. Results and discussion

3.1. Classification accuracy

The best results were obtained with the model composed of the original bands (RGB), CIVE-VDVI-NGRDI vegetation indices and Energy-Entropy textures. Classification accuracy of target species calculated from the validation dataset is presented in Figure 4. Classification models yielded a mean prediction accuracy (F1-score) of 0.90 (0.87 to 0.92) at S-P and 0.87 (0.81 to 0.91) at C-G. In this study, an accuracy of ~85% was considered sufficient to interpret the occupation changes of IPS [12].

Over the decade, the area occupied by IPS is on average 2.49 ha at S-P and 5.03 ha at C-G (Figure 4). However, the occupancy rate between S-P and C-G differs significantly, with a coefficient of variation of 3.7% and 44.7%, respectively. If the spread of IPS at S-P is low (+3.1%), the area occupied at C-G decreases highly (-42.3%), especially between 2013 and 2016. This can be explained by trees planting on cleared land previously colonized by IPS and landscape closure in some areas. Regular IPS clearing is also carried out, explaining locally their absence in some years.

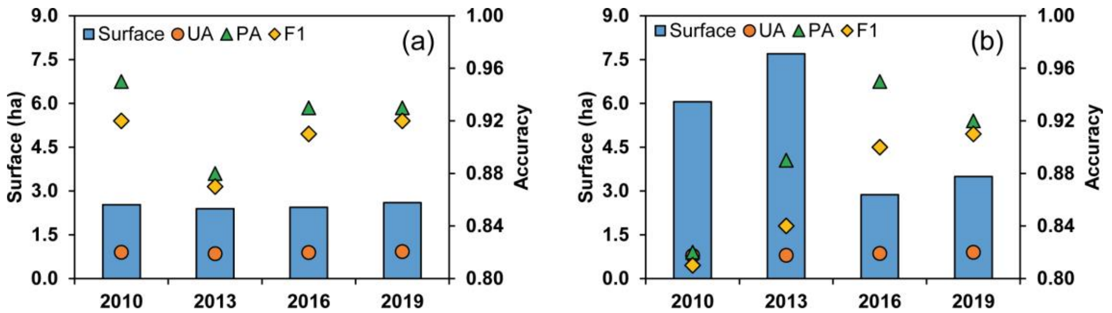

Figure 4. Evolution of the IPS areas from 2010 to 2019 and classification accuracy at Salles-et-Prat-viel (a) and Cierp-Gaud (b). 'UA', User Accuracy; 'PA', Producer Accuracy; 'F1', F1-score.

3.2. Spatial pattern of invasion

Classification maps allows to distinguish three types of preferential sites for the occurrence of IPS: (i) near wetlands (i.e., stream banks and ponds), (ii) along drainage ditches and (iii) along corridors (i.e., roads, power lines). Among these environments, those resulting from alteration by human activity are the most commonly observed at both sites.

Figure 5 presents the spatial pattern of IPS over the last decade at C-G where the spatial dynamic is the most important. Distribution maps show a non-random occurrence of IPS, whose dynamic appears to be mainly driven by anthropogenic factors. Thus, IPS mainly developed along a disturbance corridor that corresponds to a road associated on the east side with a drainage ditch and a power line (Figure 5 site 3). A second corridor corresponding to a power line also represents a preferential axis of colonization. Several isolated patches of IPS have also appeared locally as a results of land clearing. However, over time these patches tend to decrease due to the development of shrubs, trees and especially brambles (*Rubus fruticosus* Linn.) that lead to landscape closure (Figure 5 site 1-2).

IPS spread at both sites shows that the colonization of an environment following land clearing is fast, with the appearance of an aggregated and dense population after 2-3 years. This rapidity can be explained by a brutal removal of native vegetation creating an open space without competition between species.

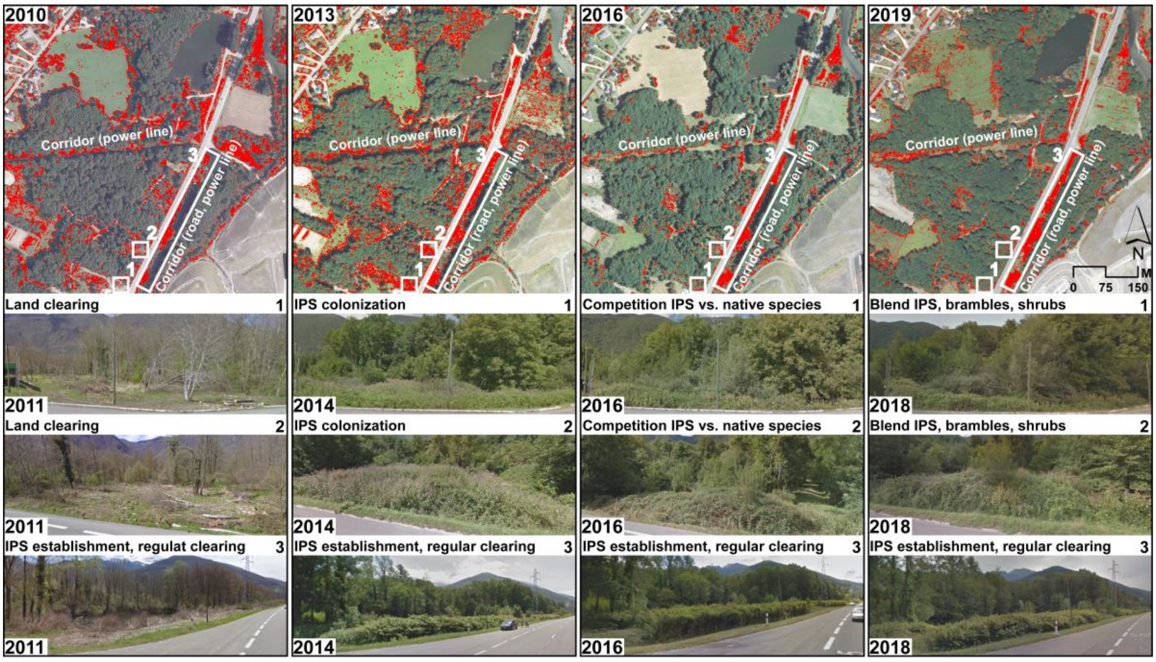

Figure 5. IPS spread pattern at Cierp-Gaud. Terrestrial images (Google Street View) illustrate the IPS temporal dynamics highlighted from the aerial images for three typical situation.

4. Conclusion

Mapping of IPS from VHR RGB images has given satisfactory results (i.e., UA and PA rates often above 85-90%) and has allowed to highlight their spatial distribution patterns. Spread of IPS can be linked to environmental and human factors that are favorable to them (i.e., wetlands, drainage ditches, corridors).

Human activity appears to play a major role in the dispersion of IPS [13], particularly through disturbance corridors (i.e., roads, power line) which generate favorable conditions for their colonization and establishment [14]. Presence of corridors leads to the removal of native species, soil disturbance, high light, modification of hydrological processes, becoming a pathway favorable for dispersal of IPS [14]. Thus, corridors generate edge effects and landscape fragmentation, leading to an abrupt transition between habitats and a modification of ecosystem with a resources redistribution and interactions among plant communities [15]. However, it appears that in some cases IPS which have colonized cleared areas (e.g., *I glandulifera*) are competing with the development of native species such as brambles and tend to lose ground.

This study identified the conditions where IPS are likely to spread. Knowing potential locations of spread and understanding the dynamic of IPS invasion can allow managers to determine the consequences of landscape changes and prioritize site-specific control strategies.

However, RGB images present low spectral resolution which can be limiting when patch size is smaller than pixel resolution or when the target is weakly distinguished from the background. Therefore, the use of multispectral images (i.e., >3 bands) acquired by unmanned aerial vehicles at sub-metric spatial resolution would improve IPS detection, especially for isolated and sparse patches. It would then be interesting to interview managers and owners about their IPS management strategies in order to clarify the interpretations of this study obtained from the image analysis.

Author Contributions: Conceptualization, H.J. and C.M.-S.; methodology, H.J. and C.M.-S.; software, H.J.; validation, H.J. and C.M.-S.; formal analysis, H.J., C.M.-S., E.M; investigation, H.J.; resources, H.B.; data curation, H.J. and S.G; writing—original draft preparation, H.J.; writing—review and editing, H.J., C.M.-S., E.M., H.B. and S.G. ; visualization, H.J.; supervision, S.G.; project administration, S.G.; funding acquisition, S.G.

Funding: This research was funded by Région Occitanie and MSH-T through the projects EI2P (grant number 19015261) and VALEEBEE (APEX 2020). This work was endorsed by the CNRS/INEE (ZA PYGAR).

Acknowledgments: The authors thank Lisa Evans for her English proofreading of the manuscript.

Conflicts of Interest: The authors declare no conflict of interest.

References

1. Vilà, M.; Hulme, P.E. *Impact of Biological Invasions on Ecosystem Services*; Springer: Cham, **2017**; ISBN 978-3-319-45121-3.
2. Vilà, M.; Ibáñez, I. Plant Invasions in the Landscape. *Landscape Ecol* **2011**, *26*, 461–472, doi:10.1007/s10980-011-9585-3.
3. Perrings, C.; Mooney, H.; Williamson, M. *Bioinvasions and Globalization: Ecology, Economics, Management, and Policy*; Oxford University Press, 2009; ISBN 978-0-19-956015-8.
4. Rejmánek, M. Invasive Plants: Approaches and Predictions. *Austral Ecology* **2000**, *25:5*, 497–506, doi:https://doi.org/10.1046/j.1442-9993.2000.01080.x.
5. Lehmann, J.R.K.; Prinz, T.; Ziller, S.R.; Thiele, J.; Heringer, G.; Meira-Neto, J.A.A.; Buttschardt, T.K. Open-Source Processing and Analysis of Aerial Imagery Acquired with a Low-Cost Unmanned Aerial System to Support Invasive Plant Management. *Front. Environ. Sci.* **2017**, *5*, doi:10.3389/fenvs.2017.00044.
6. Müllerová, J.; Pergl, J.; Pyšek, P. Remote Sensing as a Tool for Monitoring Plant Invasions: Testing the Effects of Data Resolution and Image Classification Approach on the Detection of a Model Plant Species Heracleum Mantegazzianum (Giant Hogweed). *International Journal of Applied Earth Observation and Geoinformation* **2013**, *25*, 55–65, doi:10.1016/j.jag.2013.03.004.
7. Beerling, D.J. The Effect of Riparian Land Use on the Occurrence and Abundance of Japanese Knotweed Reynoutria Japonica on Selected Rivers in South Wales. *Biological Conservation* **1991**, *55*, 329–337, doi:10.1016/0006-3207(91)90036-9.Cc
8. Pyšek, P.; Prach, K. Invasion Dynamics of Impatiens Glandulifera — A Century of Spreading Reconstructed. *Biological Conservation* **1995**, *74*, 41–48, doi:10.1016/0006-3207(95)00013-T.
9. Haralick, R.M.; Shanmugam, K.; Dinstein, I. Textural Features for Image Classification. *IEEE Transactions on Systems, Man, and Cybernetics* **1973**, *SMC-3*, 610–621, doi:10.1109/TSMC.1973.4309314.
10. Breiman, L. Random Forests. *Machine Learning* **2001**, *45*, 5–32, doi:10.1023/A:1010933404324.
11. Powers, D.M.W. Evaluation: From Precision, Recall and F-Factor to ROC, Informedness, Markedness & Correlation. J. Mach. Learn. Technol. **2011**, 2, 37–63.
12. Foody, G.M. Status of Land Cover Classification Accuracy Assessment. *Remote Sensing of Environment* **2002**, *80*, 185–201, doi:10.1016/S0034-4257(01)00295-4.
13. Hastings, A.; Cuddington, K.; Davies, K.F.; Dugaw, C.J.; Elmendorf, S.; Freestone, A.; Harrison, S.; Holland, M.; Lambrinos, J.; Malvadkar, U.; et al. The Spatial Spread of Invasions: New Developments in Theory and Evidence. *Ecology Letters* **2005**, *8*, 91–101, doi:https://doi.org/10.1111/j.1461-0248.2004.00687.x.
14. Theoharides, K.A.; Dukes, J.S. Plant Invasion across Space and Time: Factors Affecting Nonindigenous Species Success during Four Stages of Invasion. *New Phytol* **2007**, *176*, 256–273, doi:10.1111/j.1469-8137.2007.02207.x.
15. Paz-Kagan, T.; Silver, M.; Panov, N.; Karnieli, A. Multispectral Approach for Identifying Invasive Plant Species Based on Flowering Phenology Characteristics. *Remote Sensing* **2019**, *11*, 953, doi:10.3390/rs11080953.